

Polymer Chemistry

Accepted Manuscript



This is an *Accepted Manuscript*, which has been through the Royal Society of Chemistry peer review process and has been accepted for publication.

Accepted Manuscripts are published online shortly after acceptance, before technical editing, formatting and proof reading. Using this free service, authors can make their results available to the community, in citable form, before we publish the edited article. We will replace this *Accepted Manuscript* with the edited and formatted *Advance Article* as soon as it is available.

You can find more information about *Accepted Manuscripts* in the [Information for Authors](#).

Please note that technical editing may introduce minor changes to the text and/or graphics, which may alter content. The journal's standard [Terms & Conditions](#) and the [Ethical guidelines](#) still apply. In no event shall the Royal Society of Chemistry be held responsible for any errors or omissions in this *Accepted Manuscript* or any consequences arising from the use of any information it contains.

ARTICLE

Dye immobilization in halochromic nanofibers through blend electrospinning of a dye-containing copolymer and polyamide-6

Cite this: DOI: 10.1039/x0xx00000x

Received 00th January 2012,
Accepted 00th January 2012

DOI: 10.1039/x0xx00000x

www.rsc.org/

Iline Steyaert,^{†, a, c} Gertjan Vancoillie,^{†, b} Richard Hoogenboom,^{*, b} and Karen De Clerck ^{*, a}

‘Smart’ materials can be defined as materials that respond to a certain stimulus with a change in their properties. A specific class herein are halochromic textiles, *i.e.* fibrous materials that change color with pH. Such halochromic textiles play an important role in the continuous monitoring and visual reporting of the pH with applications in various fields, such as wound treatment and protective clothing. pH-sensitive nanofibrous nonwovens have high sensitivity and a fast response time, and are mostly fabricated by introducing a pH-responsive dye via dye-doping of the feed mixture before fabrication. However, this method suffers from leaching of the dye, which is an undesirable effect that not only reduces the output signal strength but can also be detrimental to the environment by causing, for instance, toxicological responses. In this paper, a new strategy is demonstrated for the reduction of dye leaching in electrospun, nanofibrous materials. Through blend electrospinning of polyamide-6 (PA6) with a dye-functionalized copolymer, large sheets of uniform, halochromic nanofibrous material can be fabricated showing a fast pH-sensitive color change. Polymeric entanglements within the nanofiber are proposed to immobilize the dye-functionalized copolymer in the PA6 matrix, resulting in drastically reduced dye leaching. Such stable nanofibrous, PA6-based, halochromic materials are particularly interesting in the design of new colorimetric sensors applicable in several sectors, including the biomedical field, agriculture, safety and technical textiles.

Introduction

The fabrication of so-called ‘smart’ materials, *i.e.* materials that change their properties in response to an external stimulus, has fascinated researchers for decades. A wide variety of polymeric materials that respond to different stimuli, such as temperature, light and concentration of a chemical substance, have been developed. This variety of different ‘smart’ materials enabled a large number of applications in various fields including drug delivery, sensing and self-healing. The development of smart colorimetric materials that sense the concentration of a specific analyte by a change in absorbance is particularly interesting, since it results in a color change directly visible to the naked eye [1-6]. The straightforward application and unambiguous output signal of these sensors make them a very powerful tool for the continuous monitoring and fast visualization of a chosen analyte. The majority of these chemical sensors incorporate analyte-sensitive dye molecules, inducing a change in optical properties under the influence of numerous stimuli including ions, gasses and a wide range of volatile organic compounds (VOC’s) [7-14].

Among colorimetric sensor materials, color-changing textiles play a prominent role. These lightweight materials show high flexibility, reusability, mechanical stability, breathability and washability. Furthermore, they can cover a large surface while still providing a local signal in a non-destructive way. Several stimuli can easily be visualized, with research mostly focusing on thermo- and photochromism. However, the less exploited halochromism, *i.e.* pH-sensitivity, may be of great value for various textile applications in the biomedical field, agriculture, safety and technical textiles since pH plays a major role in wound healing, crop growth and filter performance [15]. A fast and easy-to-interpret colorimetric signal would, therefore, be beneficial for the optimization of the working conditions or as a warning signal when incorporated into protective clothing for the detection of acid vapors.

In the search for high-performing textile sensors, electrospun nanofibers show great potential due to their unique properties linked to the nanoscale diameters; small pore size, large specific surface area and high porosity [16]. These characteristics lead to improved sensor sensitivity and response time [17-22], as well as other benefits for several applications,

such as enhanced filtration performance [23] or stimulated wound healing [18,24]. For the production of nanofibrous materials, solvent electrospinning is most commonly applied as it provides a relatively simple process to produce nanofibers from polymer solutions. Using this technique, continuous fibers with controlled diameters down to sub-100 nanometer scales can be produced through the application of electrostatic forces [16,25].

A frequently used strategy for nanofiber functionalization is the addition of low molar mass components or nanoparticles to the electrospinning solution prior to fiber formation, *i.e.* doping, including dye-doping for colorimetric pH-sensing [22-37]. Although this technique results in easy-to-produce halochromic nanofibers, the dye is only loosely retained within the fiber by the surrounding, entangled polymers. This results in a large effect of the fiber swelling in moist environments on the mobility of the dye molecule, making dye leaching a severe drawback of this method [38]. Up until now, this problem is being countered by reducing the dye mobility, mainly through application of polymeric complexing agents, which is not applicable to all dyes, however [36,37].

In this work an alternative approach is proposed to reduce dye leaching based on drastic reduction of the dye mobility within the nanofibers by incorporating it into a copolymer before fiber fabrication. This strategy provides a covalent linkage of the dye to the matrix, which appears to be the most efficient immobilization method [7,39-42]. For the design of such a functional copolymer with covalently coupled pH-sensitive dye molecules, several strategies can be followed [12,43-45]. One of the most straightforward procedures is the dye-monomer approach where the dye is functionalized with a polymerizable group and subsequently copolymerized with a suitable comonomer. This allows for excellent control of the copolymer composition, *i.e.* the amount of dye, and large-scale synthesis through economically important polymerization techniques such as free radical polymerization. In the current paper, a model system was chosen based on *N*-ethyl-*N*-(2-hydroxyethyl)-4-(4-nitrophenylazo)aniline, more commonly known as Disperse Red 1 (DR1). DR1 is a diazobenzene-based dye that is commercially available and represents dye classes not suitable for complexation with the polymeric agents used to counter dye leaching. Moreover, DR1 has a functional group that can easily be functionalized in high yields and that is isolated from the conjugated system, limiting the effect of the functionalization on the pH-responsivity [46-48].

The subsequent incorporation of the formed dye-containing copolymer into a nanofibrous product can easily be achieved using blend electrospinning. Blend electrospinning is an emerging technique for the production of high-value, functional nanofibrous materials [49,50], including nanofibers for optical sensor applications [21,51-53]. The copolymer is directly mixed with a carrier polymer in the electrospinning solution prior to fiber fabrication. Polymeric entanglements within the nanofiber are proposed to immobilize the dyed copolymer in the nanofibrous matrix, resulting in drastically reduced dye leaching. This method has several advantages: (1) the carrier

polymer can be chosen according to the applications, (2) the amount of the functional copolymer can be minimized for economical purposes and (3) the electrospinnability of the pure functional copolymer is less important since this is mainly provided by the carrier polymer.

Within this paper, electrospinnability, halochromic behavior and dye migration were investigated for a model system, namely DR1-containing nanofibers produced through blend electrospinning of polyamide-6 (PA6) as carrier polymer, and a DR1-functionalized copolymer of 2-hydroxyethyl acrylate (HEA) and DR1-acrylate (DR1-A). Our results indicate that the proposed approach results in halochromic nanofibers with minimal dye leaching. This proof-of-concept is a major step forward in the design of robust halochromic nanofibers.

Experimental

Instruments & Materials

Acryloyl chloride (97.0, MEHQ stabilizer), Disperse Red 1 (95 %) and 2-hydroxyethyl acrylate (96%, hydroquinone as inhibitor) were bought from Sigma-Aldrich. Triethylamine and dichloromethane (HPLC grade) were also obtained from Sigma-Aldrich and dried over calcium hydride. *N,N*-Dimethylacetamide (DMAc, HPLC grade) was purchased from Sigma-Aldrich and used as received. 2-Hydroxyethyl acrylate (HEA) was filtered over aluminum oxide (neutral, deactivated) to remove inhibitor, azobisisobutyronitrile (AIBN) was recrystallized from methanol. Deuterated solvents (MeOH-d₄ and DMSO-d₆) were supplied by Cambridge Isotope Laboratories, inc.

Polyamide 6 (M_w 51,000 g.mol⁻¹, \bar{D} 1.82), poly (diallyldimethylammonium chloride) (M_w 100,000 – 200,000, 20 wt% aqueous solution), acetic acid (99.8 v%) and formic acid (98-100 v%) were supplied by Sigma-Aldrich and used as received. For the preparation of pH baths, hydrochloric acid, sodium hydroxide and potassium nitrate are used, also supplied by Sigma-Aldrich. Adjacent reference fabrics (polyamide and wool) for dye migration tests were purchased from James Heal and meet the requirements of standard ISO 105-F03 and ISO 105-F01 respectively.

Synthesis of Disperse Red 1 – Acrylate (DR1-A)

This dye-functionalized monomer was prepared following an adapted literature procedure [54]. Disperse Red 1 (5.09 g, 0.016 mol, 1 eq) was dissolved in triethylamine (7.7 ml, 0.055 mol, 3.4 eq, anhydrous) and CH₂Cl₂ (250 ml, anhydrous) and cooled to 0°C under argon atmosphere. Acryloyl chloride (2.56 ml, 0.032 mol, 2 eq) was added drop wise under vigorous stirring after which the mixture was allowed to warm up to room temperature. The reaction was monitored using TLC 5/1 CH₂Cl₂/EtOAc (R_{f,DR1} = 0.50, R_{f,DR1-A} = 0.90), which revealed complete conversion after 12h. The compound was further purified using a short silica filter column with 5/1 CH₂Cl₂/EtOAc as eluent. After drying of the organic phase with MgSO₄ the solvent was evaporated, resulting in 5.69 g (95%) of

the desired DR1-A as red powder. $^1\text{H-NMR}$ (300 MHz, CD_2Cl_2 , ppm) δ_{H} : 8.24 (2H, d, $^3J = 9.33$ Hz, H_a), 7.84 (4H, dd, $^3J = 8.23$ Hz, H_b), 6.76 (2H, d, $^3J = 9.88$ Hz, H_c), 6.31 (1H, dd, $^3J = 17.56$ Hz, $^2J = 2.19$ Hz, H_d), 6.05 (1H, dd, $^3J = 18.66$ Hz, $^3J = 10.42$ Hz, H_e), 5.78 (1H, dd, $^3J = 10.42$ Hz, $^2J = 2.19$ Hz, H_f), 4.30 (2H, tr, $^3J = 5.49$ Hz, H_g), 3.66 (1H, tr, $^3J = 5.49$ Hz, H_h), 3.47 (2H, quad, $^3J = 6.58$ Hz, H_i), 1.18 (3H, tr, $^3J = 7.68$ Hz, H_j).

Synthesis of P(HEA-co-DR1-A)

A copolymer of HEA and DR1-A was synthesized using free radical copolymerization (FRP) initiated by AIBN. The solution polymerization was carried out in DMAc with a $[\text{M}]_{\text{tot},0}$ of 1 M and $[\text{HEA}]/[\text{DR1-A}]/[\text{AIBN}]$ ratio of [99]/[1]/[1]. 10 ml of HEA and 0.32 g of DR1-A were dissolved in 78 ml of DMAc. The mixture was degassed by bubbling Ar for 30 min while stirring, after which 0.14 g of AIBN was added as a solid. The mixture was homogenized and heated to 71 °C for 24 h. The reaction was stopped by cooling down the mixture and the polymer was precipitated twice in cold diethylether to obtain a red powder.

Characterization of P(HEA-co-DR1-A)

Size-exclusion chromatography (SEC) was performed on a Agilent 1260-series HPLC system with two PLgel 5 μm mixed-D columns in series heated to 50 °C and two detectors: a 1260 diode array detector (DAD) and a 1260 refractive index detector (RID) at 55°C. DMAc containing 50mM of LiCl was used as eluent at a flow rate of 0.593 ml/min. The spectra were analyzed using the Agilent Chemstation software with the GPC add on. Molar mass and dispersity (\bar{D}) values were calculated against PMMA standards from PSS. Nuclear magnetic resonance (NMR) spectra were recorded on a Bruker Avance 300 MHz spectrometer at room temperature in deuterated solvents. The chemical shifts are given relative to TMS. Conversions were calculated using the ratio between the residual acrylate peaks at 6.5 – 8.5 ppm ($\sim[\text{M}]_t$) and the methylene group adjacent to the ester group in the side chain at 4.17 ppm. The latter was integrated to include both the broad polymer and residual monomer peak, therefore correlating to $[\text{M}]_0$. More information can be found in the Electronic Supporting Information (ESI1).

Quantification of polymer hydrolysis under basic and acidic conditions

100 mg of P(HEA-co-DR1-A) was dissolved in 2 ml of pH 13 buffer solution and stirred at room temperature. A sample of 50 μl was taken and diluted with 450 μl MeOH for gas chromatography (GC) analysis at certain time intervals to determine the ethylene glycol peak at 1.67 min. The percentage of degradation was then approximated using a calibration curve and the absolute molecular weight was calculated from conversion based on $^1\text{H-NMR}$ spectroscopy.

100 mg of P(HEA-co-DR1-A) was dissolved in 1 ml of a acetic acid/formic acid 1/1 mixture and stirred at room temperature. GC samples that were prepared as previously described did not

reveal any measurable amount of ethylene glycol. This test was repeated using SEC with UV detection ($\lambda_{\text{max}} = 490$ nm) on 100 μl samples directly diluted in 900 μl DMAc + LiCl. More information on both tests can be found in the Electronic Supporting Information (ESI2).

GC was performed on an Agilent 7890A system equipped with a VWR Carrier-160 hydrogen generator and an Agilent HP-5 column of 30 m length and 0.320 mm diameter. An FID detector was used and the inlet was set to 250 °C with a split injection of ratio 25:1. Hydrogen was used as carrier gas at a flow rate of 2 mL/min. The oven temperature was increased with 20°C/min from 50°C to 120°C, followed by a ramp of 50°C/min to 300 °C.

Electrospinning procedure

The nanofibrous materials were produced by solvent electrospinning using a 50/50 acetic acid/formic acid (AA/FA) solvent system. All solutions contained a total of 16 wt% polymer. Pure PA6 solutions were electrospun as reference, dye-doped samples were obtained by adding DR1 or DR1-A directly to the PA6 electrospinning solution, and the blend nanofibers were obtained by electrospinning a solution containing 85/15 PA6/P(HEA-co-DR1-A). All colored nanofibrous nonwovens (dye-doped or blend) contained a dye concentration of either 0.5 or 0.64 % on mass fiber (%omf). The effect of the complexing agent poly (diallyldimethylammonium chloride) (PADC) was tested for a concentration of 4 %omf, also added directly to the electrospinning solution.

Prior to electrospinning, the solutions were characterized. Viscosity was measured using a Brookfield viscometer LVDV-II, conductivity was determined by a CDM210 conductivity meter (Radiometer Analytical) and surface tension was determined using the Wilhelmy plate method. The average errors for these measurements were 8%, 11% and 2% respectively.

The nanofibrous nonwovens were electrospun on a multinozzle setup, with 18 gauge needles (inner diameter of 0.838 mm), a tip-to-collector distance of 4.5 cm and a flow rate of 2 ml/h. The applied voltage was adapted to allow for a stable electrospinning process, ranging from 15 to 30 kV. All the electrospinning trials were performed at a relative humidity of $48 \pm 5\%$ and a temperature of $20 \pm 1^\circ\text{C}$.

Characterization of the electrospun samples

Fiber morphology of the electrospun structures was examined using a scanning electron microscope (FEI Quanta 200 F) at an accelerating voltage of 20 kV. Sample preparation was done using a gold sputter coater (Balzers Union SKD 030). The nanofiber diameters were measured using UTHSCSA ImageTool version 3.0, developed by the University of Texas Health Science Center. The average fiber diameters and their standard deviations are based on 50 measurements per sample. Color measurements were performed using a Perkin-Elmer Lambda 900 spectrophotometer, which is a double-beam UV-Vis spectrophotometer. For the transmission spectra of

solutions 1 cm matched quartz cells were used, for the reflection measurements on fabrics an integrated sphere (Spectralon Labsphere 150 mm) was used. The spectra were recorded from 380 nm to 780 nm with a data interval of 1 nm (transmission) and 4 nm (reflection). Transmission and reflection are converted into absorbance (A) and Kubelka-Munk (K-M) resp. since these values provide a correlation with dye concentration.

Analysis of the dye migration/immobilization was done in two different ways. Firstly, the leaching in an aqueous solution of a certain pH was tested by introducing 5 mg of fabric in a bath of 5 ml. After 24 hours, the dye migration to the aqueous bath is determined through UV-Vis spectroscopy (absorbance A). Secondly, the dye transfer to reference fabrics was tested based on the standard ISO 105-E01:1994. This standard was formulated for conventional fabrics and adapted for nanofibrous samples in this study. The nanofibrous sample is placed between two adjacent reference fabrics showing affinity for the dye, in our case PA6 on one side and wool on the other side. While in contact with these reference fabrics, the nanofibrous sample is immersed in an aqueous solution of certain pH for 30 minutes and, subsequently, placed in an oven (37°C) under a calibrated load for 4 hours. The staining of the adjacent reference fabrics is characterized by UV-Vis spectroscopy, obtaining the Lab-values (OptLab-SPX, 10° observer, D65 illuminant). Based on these values, a color difference (ΔE) is calculated between the unstained and the stained reference, giving an effective measure of the dye migration to the adjacent fabrics. A detailed description of the calculation of a color difference (ΔE) can be found in the Electronic Supporting Information (ESI4). Results are discussed using the staining of the PA6 reference fabrics. Exactly the same trends were recorded for the wool reference fabrics.

For the characterization of halochromic behavior and leaching of the dye, the pH of the aqueous solutions was determined using a combined reference and glass electrode (SympHony Meters VMR) while hydrochloric acid and sodium hydroxide were used to adjust the pH.

Results and discussion

Synthesis of dye-functionalized polymer

The primary alcohol in DR1 is an excellent functionalization position because of its nucleophilicity and isolation from the conjugated system, limiting the effect of the functionalization on the color and pH-shift of the dye. By using an excess of acryloyl chloride and triethylamine, the reaction reaches complete conversion, which simplifies the larger scale work-up. The product can easily be purified by flash chromatography on a short silica column using a DCM/EtOAc 5/2 solvent mixture as only DR1-A will run under these conditions. Using this method, up to 10 grams of dye can be synthesized and isolated from a single reaction with yields exceeding 95 %.

Since the electrospinning experiments demand several grams of copolymer, free radical polymerization (FRP) was chosen as polymerization technique for its simplicity and effectiveness during multi gram polymerizations. The resulting copolymers show a relatively broad molecular weight distribution

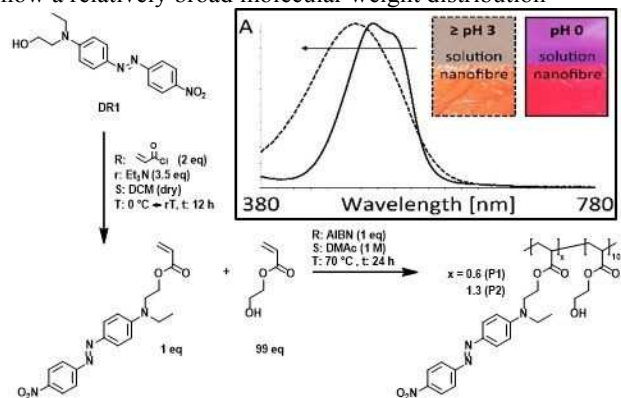


Fig. 1: Chemical structure, reaction mechanism and polymerization conditions of P(HEA-co-DR1-A). Inset: pH-responsive behavior of P(HEA-co-DR1-A) in aqueous solution (top) and nanofiber (bottom).

characterized by a \bar{M}_w of slightly higher than two, which is common for an uncontrolled (free) radical polymerization. An added advantage of FRP is the high monomer conversion, limiting the waste of the expensive DR1-A monomer. The hydrophilic 2-hydroxyethyl acrylate (HEA) was chosen as base comonomer, as it is hydrophilic and small. Its small size will minimize any shielding effect of the dye by the polymer and thus, in combination with its hydrophilicity, ensure excellent contact between dye and the changing aqueous environment. Two batches of the copolymer were synthesized using the same conditions and ratios but differing in scale. The large-scale polymerization of 20 ml HEA showed a conversion of 98% after 24 h at 70°C as measured using $^1\text{H-NMR}$ spectroscopy. After precipitation of the polymer, the UV-signal on the SEC analysis confirmed the incorporation of DR1 into the polymer structure and complete removal of unreacted DR1-A. From the RI-signal, a M_n of 22,000 Da and a \bar{M}_w of 2.20 were calculated. $^1\text{H-NMR}$ spectroscopy of the purified copolymer also confirmed the complete removal of residual DR1-A and allowed the calculation of the actual copolymer composition. Based on the integration of one aromatic signal of DR1 ($\delta = 8.38$ ppm) and the methylene groups adjacent to the ester moiety in both side chains ($\delta = 4.16$ ppm), the percentage of incorporated DR1-A was calculated to be 0.6 mol%. A second, smaller batch of copolymer was synthesized using 10 ml HEA and characterized using the same procedures. This batch had a similar conversion of 98% but had a significantly smaller M_n of 13,000 Da ($\bar{M}_w = 2.13$). These differences can be explained by the uncontrollability of the used polymerization technique, possibly in combination with the larger influence of residual oxygen on smaller scale and/or the presence of chain transfer inducing impurities (amines) in the DMAc used for the second batch. All other copolymer batches that were synthesized

showed characteristics similar to P1. Despite the unknown origin of its lower molar mass, the second batch was used to investigate the influence of a lower Mn and higher dye content on the electrospinning process and resulting dye immobilization.

Table 1. Characterization data of the used dye-copolymer batches.

	Conv HEA	Mn (Da)	Đ	DR1-A content
P1	98 %	22,000	2.20	0.6 mol%
P2	98 %	13,000	2.13	1.3 mol%

Electrospinning of the halochromic nanofibers

The electrospinnability of the PA6/P(HEA-co-DR1-A) blend was studied in function of processing conditions, process stability and resulting fiber morphology and compared to pure and dye-doped PA6 solutions. It is well known that the addition of low molar mass components or a second polymer component may alter these parameters significantly [55,56]. To study the effect of added DR1, DR1-A and P(HEA-co-DR1-A) on the electrospinning process, several other crucial parameters were fixed, including solvent system (50/50 AA/FA), polymer concentration (16wt%), blend ratio (85/15 PA6/P(HEA-co-DR1-A)), tip-to-collector distance (4.5 cm) and flow rate (2 ml/h). All the electrospinning trials were performed in a climate-controlled lab (48% RH \pm 5% and 20°C \pm 1°) so that the known influence of relative humidity (RH) on fiber morphology [57] is minimal. The applied voltage was adjusted for each experiment to obtain a stable process (in between 20-30 kV).

Table 2. Characterization data of the used electrospinning solutions.

	Conductivity [mS/cm] \pm 10%	Viscosity [mPa.s] \pm 10%	Surface tension [mN/m] \pm 3%
PA6	0.575	529	31
PA6/DR1	0.632	574	33
PA6/DR1-A	0.656	544	32
PA6/P1*	0.577	481	32

* blend solution containing 85/15 PA6/P(HEA-co-DR1-A) of batch P1

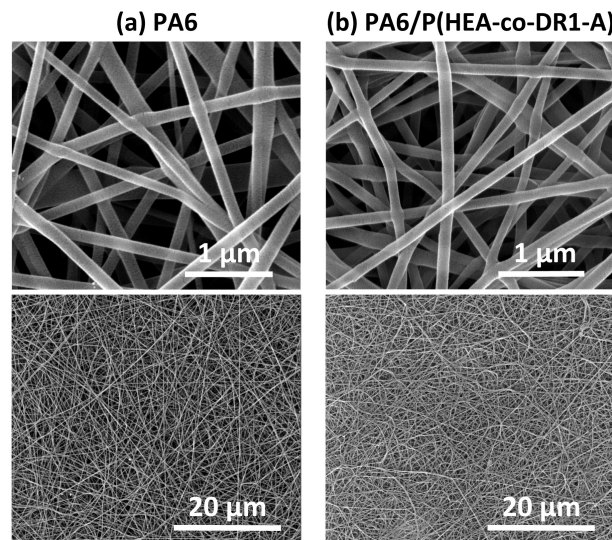


Fig. 2: SEM-images of the pure PA6 nanofibers (a), having a fiber diameter of 136 ± 19 nm, and the blend nanofibers (b), having a fiber diameter of 138 ± 25 nm. Fiber morphology is comparable; uniform, beadless nanofibers are formed.

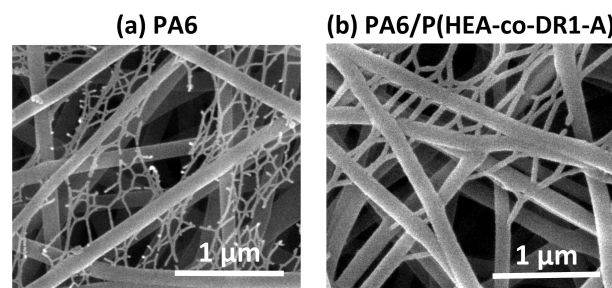


Fig. 3: SEM-images of the pure PA6 nanofibers (a) and the blend nanofibers (b), both showing some nanoweb formation.

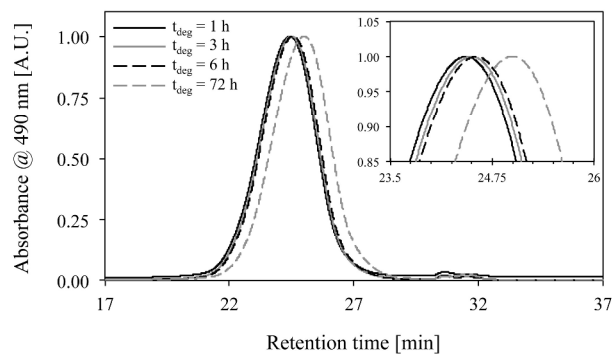


Fig. 4: Normalized SEC traces, measured with a DAD detector at 490 nm show a small decrease in molecular weight of P(HEA-co-DR1-A) in the acetic acid/formic acid solvent system over time, illustrated by the increase in retention time. Inset: zoomed region of interest near the peak molecular weight.

Incorporation of DR1 or DR1-A did not significantly change any solution parameters (Table 2) and was found to have no significant effect on the processing conditions and process stability, nor the fiber morphology when compared to pure PA6, which is in agreement with literature [36,28]. SEM-analysis shows that homogeneous fibers without droplets or beads are formed (ESI3). The PA6/P(HEA-co-DR1-A) blends were also found to be electrospinnable without any profound changes in processing conditions or stability, resulting in uniform, beadless nanofibers (Fig. 2b compared to Fig. 2a). The SEM-images in Fig. 2b are of PA6/copolymer P1 blend nanofibers (details P1 in Table 1). SEM-images of the PA6/copolymer P2 blend nanofibers were similar, indicating that there is no significant influence of the polyacrylate molar mass within this range.

Similar to other polymers already reported in literature [58], small nanofibers in between the main nanofibrous nonwoven could be found in all our samples (Fig. 3). These smaller fibers are referred to as nanowebs and mostly have diameters an order of magnitude smaller than the main nanofibers acting as support. The blend solutions were more sensitive to nanoweb formation than the pure and dye-doped PA6 solutions, especially in the start-up phase of the electrospinning process. Ding et al. describe that high solvent evaporation rates and fast phase separations can induce nanoweb formation [59]. Electrospinning a polymer blend in the vapor-poor atmosphere of the start-up phase of the process could render the system more sensitive to phase separation, possibly explaining the more pronounced nanoweb formation during start-up. Overall, the polymer blends were well electrospinnable, resulting in blend nanofibers with diameters comparable to the pure PA6 nanofibers (138 ± 25 nm and 136 ± 19 nm, respectively).

In addition to the electrospinnability, the long-term process stability was also investigated. It is well known that PA6 is electrospinnable using the chosen solvent system (acetic acid/formic acid) and long-term process stability is guaranteed [57]. Solubilizing P(HEA-co-DR1-A) in these harsh conditions for a prolonged time might influence the polymer structure through degradation, possibly resulting in different electrospinnability or fiber morphology during extended spinning periods as the polymer mixture is dissolved in the AA/FA mixture (diameter, nanoweb, etc.). In order to quantify this potential degradation, 100 mg of P(HEA-co-DR1-A) was dissolved in 1 ml of a 50/50 AA/FA mixture and stirred at room temperature. This polymer solution was sampled in time and measured with size exclusion chromatography (SEC). Fig. 4 shows the SEC traces (absorbance @ 490 nm) obtained after different times, indicating minor polymer degradation as shown by the slight shift of the polymer peak towards higher retention times. The shift, however, is very small and, in agreement, the

electrospinning trials at different moments for over 3 days indicated similar electrospinning behavior and fiber morphology. This demonstrates that the small decrease in molecular weight of the polyacrylate component does not significantly influence the electrospinning process. Blend electrospinning of P(HEA-co-DR1-A) with PA6 as carrier polymer, is thus a viable method for producing nanofibers containing covalently bonded pH-sensitive dye molecules.

pH-sensitivity of the halochromic nanofibers

Similar to the dye-doped nanofibers (DR1 and DR1-A), the blend nanofibers show a clear color change with increasing pH from bright pink at pH 0 to orange at pH > 1 as previously shown in Fig. 1. Importantly, this is a reversible and fast color change, not only observed in aqueous media but also when exposed to hydrochloric acid vapors, making these materials interesting for a wide range of applications, including protective 'smart' clothing. A quantitative characterization of this halochromic behavior is possible through UV-Vis spectroscopy, as shown in Fig. 5. The nanofibrous samples were immersed in water baths with pH varying between 0 and 12 prior to the measurement. Normalized Kubelka-Munk spectra of the samples show that all samples have a similar color change due to a shift to lower wavelengths, *i.e.* a hypsochromic shift, with increasing pH going from a maximum around 515 nm to a maximum around 495 nm (Fig. 5a-c). Additionally, at higher pH values the shoulder, visible at low pH around 545 nm, disappears. Not only the color change, but also the pH-range is similar for all nanofibrous samples with sensitivity mainly between pH 0 and pH 1. Also the third aspect of halochromic behavior, namely response time, is comparable for all nanofibrous samples. Within a few seconds, the samples gain their final color, characteristic of the pH of the environment. Van der Schueren et al. determined that wettability of the nanofibrous samples, which is coupled to the hydrophilicity of the polymer components, is a major determining factor in the sensor response time [37]. Both PA6 and the dye-copolymer are hydrophilic (co)polymers and thus wettability of the samples is excellent, giving rise to fast-responsive halochromic nanofibers.

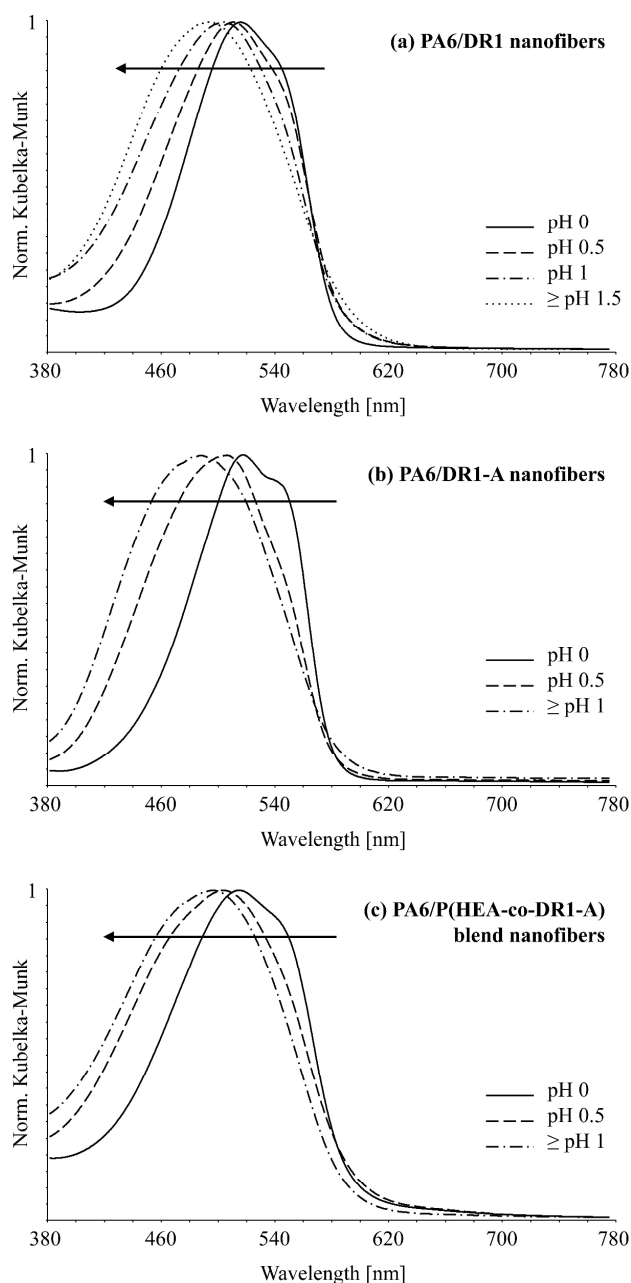


Fig. 5: Normalized Kubelka-Munk values of the DR1-doped (a), DR1-A-doped (a) and blend (c) nanofibrous samples, illustrating the color change from bright pink to orange through a hypsochromic shift with increasing pH. No significant differences in halochromic behavior are registered between the samples.

Optical properties of indicator dyes can be very sensitive to the environment (matrix) and immobilization reactions [7,10,20]. As anticipated, the latter did not significantly affect the halochromic behavior of DR1, since the functionalization is performed at the hydroxyl group that is electronically decoupled from the conjugated dye system (chromophore). Indeed, both the DR1-A-doped nanofibers and the P(HEA-co-DR1-A)-containing nanofibers have similar properties to the DR1-doped nanofibers, as described above. DR1 is an azo dye

best known for its applications in electro-optics or solvatochromism. Its halochromic properties are less exploited since the dye is not easily soluble in aqueous solutions, especially at higher pH in its unprotonated state. P(HEA-co-DR1-A), however, is well soluble in water at room temperature, allowing us to evaluate the influence of the PA6 nanofibrous environment on the halochromic properties of the dye, compared to an aqueous environment (Fig. 6a vs. Fig. 6b).

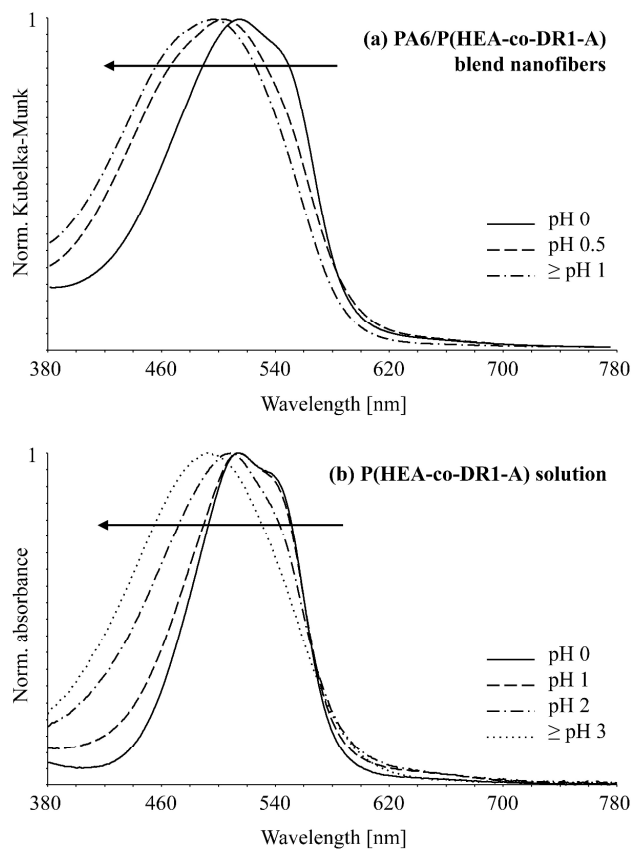


Fig. 6: Normalized Kubelka-Munk values of the blend nanofibrous sample (a) and normalized absorbance spectra of an aqueous P(HEA-co-DR1-A) solution (b). Interactions between the dye-copolymer and PA6 in the nanofibers have a small influence on the halochromic behavior; the pH-range of the color change is narrowed and shifted to lower pH values.

The color change in both environments is similar, going from bright pink to pale orange. The polymer environment, however, affects the pH-range in which the color change takes place, shifting it to lower pH values for the nanofibers in comparison to the aqueous solution. Specific interactions between DR1 and PA6, possibly including hydrogen bonding and ionic interactions, apparently cause a decrease in pKa of DR1 from around 1.5 in aqueous solution to about 0.5 in the nanofibrous environment. Similar to the effect of substituents on the dye chromophore more frequently studied in literature [61,62], it is not uncommon that incorporation of pH-indicator dyes in polymer matrices result in a shift in pKa of 1 unit due to dye-matrix interactions [7]. Overall, the changes in halochromic properties of DR1 are limited to this change in pKa, illustrating

that blend electrospinning using a DR1-containing copolymer is a viable strategy for the production of fast-responsive halochromic nanofibers.

Dye release

As previously mentioned, in the development of halochromic nanofibers the chosen indicator dye is mostly added to the electrospinning solution before fiber production, referred to as dye-doping. For most systems, there are no specific interactions between the polymer and the dye, leading to improper immobilized dye molecules and thus dye leaching, being a major for future applications [35,36,62]. Van der Schueren et al. showed that the use of a polymeric complexing agent significantly reduces the leaching of some pH-sensitive dye molecules since the mobility of the dye-polymer complex is lowered [36,37]. However, this strategy is only useful for complex-forming dye molecules. This paper therefore investigates the more generally applicable covalent linkage of the dye to a polymer component, illustrated with the DR1-based model system. The leaching is quantified by comparing dye-transfer of the DR1-containing nanofibrous samples to standardized reference fabrics after being in contact under specific conditions detailed in the experimental section. The migration of the dye was subsequently quantified by comparing the color of the reference fabrics to their unstained counterparts (Fig. 7).

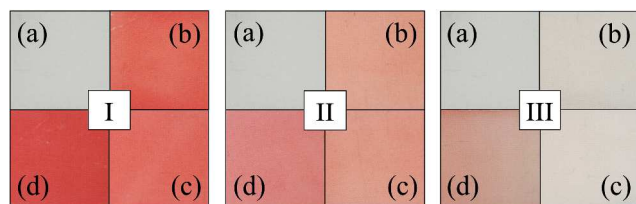


Fig. 7: Staining of the PA6 reference fabrics in the water fastness tests using (I) PA6/DR1, (II) PA6/DR1-A and (III) PA6/P(HEA-co-DR1-A) samples. The difference between the unstained reference (a) and the stained references (b: pH 2, c: pH 7, d: pH 12) is indicative for dye leaching, which is negligible for the blend nanofibers.

The results show that there is significant dye transfer from the dye-doped nanofibrous samples (both with DR1 and DR1-A) to the reference fabrics at all pH values (compare a to b, c and d resp. in Fig. 7I and 7II), whereas there is almost no staining of the reference when in contact with the blend nanofibers (compare a to b, c and d resp. in Fig. 7III). This remarkable difference in reference staining illustrates the merit of the covalent bond and efficient immobilization of P(HEA-DR1-A) in the PA6 matrix,

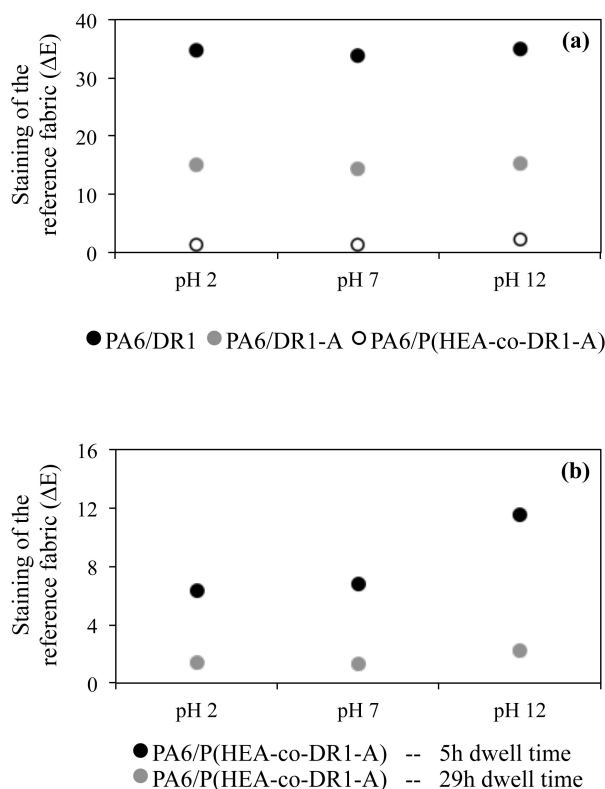


Fig. 8: Water fastness results, reflecting dye migration to a PA6 reference fabric, indicating that dye leaching is minimal for the blend nanofibers (a) and that a longer dwell time of the polymers in the acid electrospinning solution significantly lowers dye leaching (b).

proposedly by chain entanglements. What was visually represented in Fig. 7, is now quantified in Fig. 8a through calculation of the color difference ΔE between the unstained reference fabric and the stained fabrics at different pH. Introduction of an acrylate group into the DR1 dye molecule decreases ΔE by half, since the dye molecule is rendered more hydrophobic. It is clear, however, that even DR1-A is not properly immobilized in the dye-doped nanofibers as major dye migration is still observed. In contrast, blend nanofibers show an almost negligible dye migration, ascribed to fixation of the P(HEA-DR1-A) within the PA6 nanofibers through chain entanglements. For reference, also PDAC was added to the dye-doped PA6 nanofibers, but it did not result in a reduction of ΔE , illustrating the viability of the immobilization strategy based on covalent coupling of this type of dye molecule. Additionally, dye migration was even lower with longer dwell times of the PA6/P(HEA-co-DR1-A) blend in solution before fiber formation, as can be seen in Fig. 8b, possibly due to better mixing resulting in a more homogeneous electrospinning solution.

Fig. 8b also revealed a higher ΔE value at high pH for the polymer blend nanofibers. In order to investigate the effect of pH on the dye release of the blend nanofibers, additional water fastness tests were performed. The nanofibrous samples were introduced in aqueous solutions with different pH values and

after 24 hours of soaking, the absorbance values of the solutions

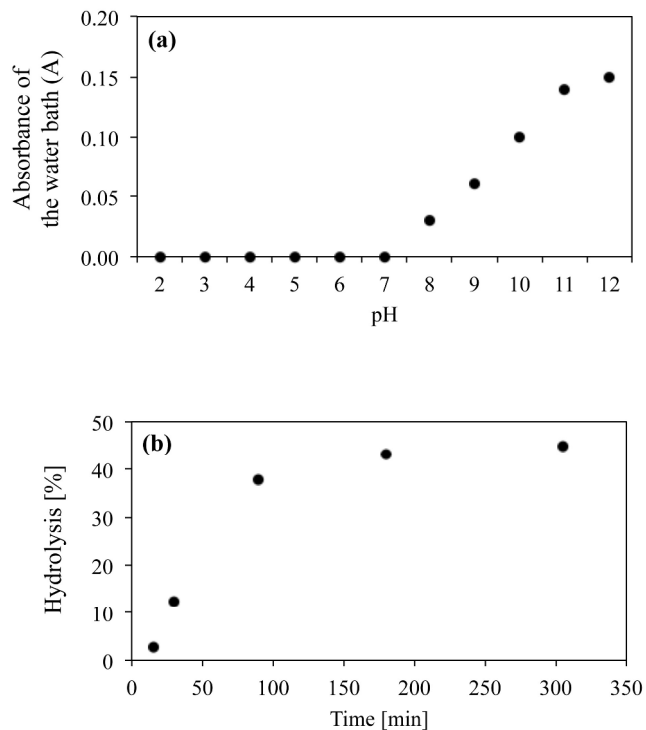


Fig. 9: (a) Water fastness results reflecting dye migration to a water bath, indicating that the blend nanofibers (29h dwell time) show increasing dye release at pH above 7, possibly due to hydrolysis and higher solubility in aqueous solution. (b) Extent of hydrolysis of P(HEA-co-DR1-A) in buffered solution at pH 13, as determined based on gas chromatography experiments measuring ethylene glycol concentrations.

were recorded, giving an effective measure of the dye concentration (Fig. 9a). At pH values above 7, the dye release to the solution systematically increased with increasing pH. SEC analysis of these solutions revealed that the measured color was caused by dissolved copolymer and not by individual DR1 molecules (ESI2), indicating that the DR1-containing copolymer dissolves out of the blend nanofibers at higher pH. In an alkaline environment, the P(HEA-co-DR1-A) that is in contact with the water can undergo hydrolysis, transforming the poly(2-hydroxyethyl acrylate) into poly(acrylic acid) under release of ethylene glycol. The resulting acrylic acid groups will be deprotonated leading to significantly enhanced solubility of the copolymer and its partial dissolution. Quantification of the speed and the extent of hydrolysis was performed by measuring the amount of ethylene glycol released in time in a buffered copolymer solution at pH 13 using gas chromatography (Fig. 9b). Initially, the amount of ethylene glycol increases quickly, indicating fast hydrolysis at this pH value. Gradually, the increase is slowed down due to neutralization of the buffer by the formed acrylic acid until it reaches a plateau at a hydrolysis percentage of roughly 45%. The hydrolysis percentage at the plateau is strongly dependent

on the starting pH of the solution, as this determines the amount of acrylic acid that needs to be formed to neutralize the solution and thereby stops the hydrolysis. This effect also explains the increase in absorbance of the water bath with increasing pH shown in Fig. 9a, as this corresponds to a higher hydrolysis percentage in the copolymer and therefore a higher solubility. In future work, this effect may be minimized by replacing the hydrolysis-sensitive acrylate monomer with a more stable methacrylate or acrylamide.

Conclusions

In summary, a new concept for the facile immobilization of pH-responsive dyes in nanofibrous nonwoven materials was demonstrated by electrospinning a mixture of PA6, as matrix material, and a DR1-functionalized P(HEA). The use of blend electrospinning allowed the fabrication of halochromic materials based on PA6 with a stable fiber diameter, homogenous color and fast local pH response. The incorporation of the dye into the copolymer drastically decreased its mobility and leaching from the fibers, proposedly due to polymer entanglements with PA6 within the nanofibers. This is concluded based on the almost negligible migration of the dye from the blend nanofibers to a reference fabric or water bath at acidic or neutral pH. These developed sensor materials are interesting for several sectors, including the biomedical field, agriculture, safety and technical textiles. Application as a visual warning patch in protective clothing could be particularly interesting as a fast and clear color change is obtained by exposure to for instance hydrochloric acid fumes. For applications in the biomedical sector, future work will involve the use of a more hydrolytically stable copolymer and a pH-responsive dye with a sensing region between the pH of 6.5-7 in order to fabricate a hydrolytically stable working example of a 'smart' wound dressing.

Acknowledgements

Financial support from The Agency for Innovation by Science and Technology of Flanders (IWT) is gratefully acknowledged. Results in this paper were obtained within the framework of the IWT Strategic Basic Research Grants 111158 and 111141. Additionally, we thank Tom De Vrieze and Konstanina Paritsi for their lab work contribution.

Notes and references

†, These authors contributed equally to the work.

^a Fibre and Colouration Technology Research Group, Department of Textiles, Ghent University, Technologiepark 907, 9052 Ghent, Belgium – +32 (0)9 264 57 40 - karen.declerck@ugent.be.

^b Supramolecular Chemistry Group, Department of Organic and Macromolecular Chemistry, Ghent University, Krijgslaan 281 S4, 9000 Ghent, Belgium – +32 (0)2 264 44 82 - richard.hoogenboom@ugent.be.

^c Research Unit of Physical Chemistry and Polymer Science, Department of Materials and Chemistry, Vrije Universiteit Brussel, Pleinlaan 2, 1050 Brussels, Belgium

Electronic Supplementary Information (ESI) available: (1) ¹H-NMR spectra and SEC traces, (2) Hydrolysis of P(HEA-co-DR1-A), (3) Electrospinning of DR1-containing nanofibers and (4) Calculation of color differences. See DOI: 10.1039/b000000x/

References

- [1] P.T. Mather, *Nature Materials*, 2007, **6**, 93
- [2] B. Adhikari, S. Majumdar, *Progress in Polymer Science*, 2004, **29**, 699
- [3] D. Roy, J.N. Cambre, B.S. Sumerlin, *Progress in Polymer Science*, 2010, **35**, 278
- [4] S-K. Ahn, R.M. Kasi, S-C Kim, N. Sharma, Y. Zhou, *Soft Matter*, 2008, **4**, 1151
- [5] I. Roy, M.N. Gupta, *Chemistry & Biology*, 2003, **10**, 1161
- [6] F. Liu, M.W. Urban, *Progress in Polymer Science*, 2010, **35**, 2
- [7] G.J. Mohr, H. Müller, B. Bussemer, A. Stark, T. Carofiglio, S. Trupp, R. Heuermann, T. Henkel, D. Escudero, L. Gonzalez, *Analytical and Bioanalytical Chemistry*, 2008, **392**, 1411
- [8] M.C. Janzen, J.B. Ponder, D.P. Bailey, C.K. Ingison, K.S. Suslick, *Analytical Chemistry*, 2006, **78**, 3591
- [9] E. Moczko, I.V. Meglinski, C. Bessant, S.A. Piletsky, *Analytical Chemistry*, 2009, **81**, 2311
- [10] C. McDonagh, C.S. Burke, B.D. MacCraith, *Chemical Reviews*, 2008, **108**, 400
- [11] G.J. Mohr, *Analytical and Bioanalytical Chemistry*, 2006, **386**, 1201
- [12] P. Makedonski, M. Brandes, W. Grahn, W. Kowalsky, J. Wihern, S. Wiese, H.-H. Johannes, *Dyes and Pigments*, 2004, **61**, 109
- [13] H. Guillemain, M. Rajarajan, Y.-C. Lin, C.-T. Chen, T. Sun, K.T.V. Grattan, *Measurement*, 2013, **46**, 2971
- [14] M. Schäferling, *Angewandte Chemie International Edition*, 2012, **51**, 3532
- [15] L. Van der Schueren, K. De Clerck, *Coloration Technology*, 2012, **128**, 82
- [16] J.H. Wendorff, S. Agarwal, A. Greiner, *Electrospinning: Materials, Processing and Applications*, 2012, Germany: Wiley-VCH Verlag & Co.
- [17] S. Chigome, N. Torto, *Analytica Chimica Acta*, 2011, **706**, 25
- [18] N. Bhardwaj, S.C. Kundu, *Biotechnology Advances*, 2010, **28**, 325
- [19] V. Thavasi, G. Singh, S. Ramakrishna, *Energy & Environmental Science*, 2008, **1**, 205
- [20] B. Ding, M. Wang, J. Yu, G. Sun, G. Sensors, 2009, **9**, 1609
- [21] X. Wang, C. Drew, S.-H. Lee, K.J. Senecal, J. Kumar, L.A. Samuelson, *Nano Letters*, 2002, **2**, 1273
- [22] L. Matlock-Colangelo, A.J. Baeumner, *Lab on a Chip*, 2012, **12**, 2612
- [23] M. Botes, T.E. Cloete, *Critical Reviews in Microbiology*, 2010, **36**, 68
- [24] Y.-F. Goh, I. Shakir, R. Hussain, *Journal of Materials Science*, 2013, **48**, 3027
- [25] S. Ramakrishna, K. Fujihara, W.-E. Teo, T.-C. Lim, Z. Ma, *An Introduction to Electrospinning and Nanofibers*, 2005, Singapore: World Scientific Publishing Co. Pte. Ltd.
- [26] R. Sahay, P.S. Kimar, R. Sridhar, J. Sundaramurthy, J. Venugopal, S.G. Mhaisalkar, S. Ramakrishna, *Journal of Materials Chemistry*, 2012, **22**, 12953
- [27] E.-M. Lee, S.-Y. Gwon, B.-C. Ji, S. Wang, S.-H. Kim, *Dyes and Pigments*, 2011, **92**, 542
- [28] Y. Ner, J.G. Grote, J.A. Stuart, G.A. Sotzing, *Soft Matter*, 2008, **4**, 1448
- [29] X. Liang, Y. Li, W. Peng, J. Bai, C. Zhang, Q. Yang, *European Polymer Journal*, 2008, **44**, 3156
- [30] F. Di Benedetto, E. Mele, A. Composeo, A. Anthanassiou, R. Cingolani, D. Pisignano, *Advanced Materials*, 2008, **20**, 314
- [31] A. Composeo, F. Di Benedetto, R. Stabile, R. Cingolani, D. Pisignano, *Applied Physics Letters*, 2007, **90**, 143115
- [32] A. Composeo, F. Di Benedetto, R. Stabile, A.A.R. Neves, R. Cingolani, D. Pisignano, *Small*, 2009, **5**, 562
- [33] D. Fantini, L. Costa, *Polymers Advanced Technologies*, 2009, **20**, 111
- [34] O.S. Wolfbeis, *Analytical Chemistry*, 2008, **80**, 4269
- [35] A. Agarwal, A. Raheja, T.S. Natarajan, T.S. Chandra, *Sensors and Actuators B: Chemical*, 2012, **161**, 1097
- [36] L. Van der Schueren, T. Mollet, Ö. Ceylan, K. De Clerck, *European Polymer Journal*, 2010, **46**, 2229
- [37] L. Van der Schueren, T. De Meyer, I. Steyaert, Ö. Ceylan, K. Hemelsoet, V. Van Speybroeck, K. De Clerck, *Carbohydrate Polymers*, 2013, **91**, 284
- [38] T.R. Dargaville, B.L. Farrugia, J.A. Broadbent, S. Pace, Z. Upton, N.H. Voelcker, *Biosensors and Bioelectronics*, 2013, **41**, 30
- [39] S. Trupp, M. Alberti, T. Carofiglio, E. Lubian, H. Lehmann, R. Heuermann, E. Yacoub-George, K. Bock, G.J. Mohr, *Sensors and Actuators B: Chemical*, 2010, **150**, 206
- [40] A. Lobnik, I. Oehme, I. Murkovic, O.S. Wolfbeis, *Analytica Chimica Acta*, 1998, **367**, 159
- [41] T. Doussineau, A. Schulz, A. Lapresta-Fernandez, A. Moro, S. Körsten, S. Trupp, G.J. Mohr, *Chemistry – A European Journal*, 2010, **16**, 10290
- [42] L. Van der Schueren, K. De Clerck, G. Brancatelli, G. Rosace, E. Van Damme, W. De Vos, *Sensors and Actuators B: Chemical*, 2012, **162**, 27
- [43] T.H. Nguyen, T. Venugopala, S. Chen, T. Sun, K.T.V. Grattan, S.E. Taylor, P.A.M. Basheer, A.E. Long, *Sensors and Actuators B: Chemical*, 2014, **191**, 498
- [44] T. Carofiglio, C. Fregonese, G.J. Mohr, F. Rastrelli, U. Tonellato, *Tetrahedron*, 2006, **62**, 1502
- [45] Q. Zhang, G. Vancoillie, R. Hoogenboom, *Thermometry at the Nanoscale*, ed. L. D. Carlos and F. Palacio, RSC publishing, Cambridge, Chapter Accepted for Publication
- [46] C. Pietsch, R. Hoogenboom, U.S. Schubert, *Angewandte Chemie International Edition*, 2009, **48**, 5653
- [47] C. Pietsch, U.S. Schubert, R. Hoogenboom, *Chemical Communications*, 2011, **47**, 8750
- [48] G. Vancoillie, S. Pelz, E. Holder, R. Hoogenboom, *Polymer Chemistry*, 2012, **3**, 1726
- [49] J. Gunn, M. Zhang, *Trends in Biotechnology*, 2010, **28**, 189
- [50] C. Tran, V. Kalra, *Soft Matter*, 2013, **9**, 846
- [51] J. Yoon, S.K. Chae, J.-M. Kim, *Journal of the American Chemical Society*, 2007, **129**, 3038

Journal Name

- [52] H. Long, H. Chen, H. Wang, Z. Peng, Y. Yang, G. Zhang, N. Li, F. Liu, J. Pei, *Analytica Chimica Acta*, 2012, **744**, 82
- [53] A. Camposeo, F. Di Benedetto, R. Cingolani, D. Pisignano, *Applied Physics Letters*, 2009, **94**, 043109
- [54] F. Kajzrat, O. Krupka, G. Pawlik, A. Mitus, I. Rau, *Molecular Crystals and Liquid Crystals*, 2010, **522**, 180
- [55] D. Li, Y. Xia, *Advanced Materials*, 2004, **16**, 1151
- [56] M. Bognitzki, T. Frese, M. Steinhart, A. Greiner, J.H. Wendorff, *Polymer Engineering and Science*, 2001, **41**, 982
- [57] S. De Vrieze, B. De Schoenmaker, Ö. Ceylan, J. Depuydt, L. Van Landuyt, H. Rahier, G. Van Assche, K. De Clerck, *Journal of Applied Polymer Science*, 2011, **119**, 2984
- [58] B. Ding, M. Wang, X. Wang, J. Yu, G. Sun, *Materials Today*, 2010, **13**, 16
- [59] B. Ding, L. Chunrong, Y. Miyauchi, O. Kuwaki, S. Shiratori, *Nanotechnology*, 2006, **17**, 3685
- [60] M.E. Cooper, S. Gregory, E. Adie, S. Kalinka *Journal of Fluorescence*, 2002, **12**, 425
- [61] T. De Meyer, K. Hemelsoet, V. Van Speybroeck, K. De Clerck, *Dyes and Pigments*, 2014, **102**, 241
- [62] L. Van der Schueren, K. Hemelsoet, V. Van Speybroeck, K. De Clerck, *Dyes and Pigments*, 2012, **94**, 443

Table of Content entry

Halochromic polyamide6-based fabrics with severely reduced dye-leaching through blend-electrospinning of PA6 with dye-functionalized copolymer.

TOC picture

